Proton Conducting Crosslinked Polymer Electrolyte Membranes Based on SBS Block Copolymer

Dong Kyu Roh, Jong Kwan Koh, Won Seok Chi, Yong Gun Shul, Jong Hak Kim

Department of Chemical and Biomolecular Engineering, Yonsei University, 262 Seongsanno, Seodaemun-gu, Seoul 120-749, South Korea

Received 7 April 2010; accepted 5 December 2010
DOI 10.1002/app.33937
Published online 11 April 2011 in Wiley Online Library (wileyonlinelibrary.com).

ABSTRACT: A series of crosslinked polymer electrolyte membranes with controlled structures were prepared based on poly(styrene-*b*-butadiene-*b*-styrene) (SBS) triblock copolymer and a sulfonated monomer, 2-sulfoethyl methacrylate (SEMA). SBS membranes were thermally crosslinked with SEMA in the presence of a thermal-initiator, 4,4′-azobis(4-cyanovaleric acid) (ACVA), as confirmed by FT-IR spectroscopy. The water uptake and ion exchange capacity (IEC) of membranes increased almost linearly with SEMA concentrations due to the increase of SO_3^- groups. However, the proton conductivity of membranes increased linearly up to 33 wt % of SEMA, above which it abruptly jumped to 0.04 S/cm presumably due to the formation of well-developed proton channels. Microphase-separated morphology and amorphous structures of crosslinked SBS/SEMA membranes were observed using wide angle X-ray scattering (WAXS), small angle X-ray scattering (SAXS), and transmission electron microscopy (TEM). The membranes exhibited good mechanical properties and high thermal stability up to 250°C, as determined by a universal testing machine (UTM) and thermal gravimetric analysis (TGA), respectively. © 2011 Wiley Periodicals, Inc. J Appl Polym Sci 121: 3283–3291, 2011

Key words: block copolymers; crosslinking; proton conductivity; ionomers; polymer electrolyte membrane

INTRODUCTION

Polymer electrolytes are materials of current interest because of their high ionic conductivity, stable electrochemical characteristics, and excellent mechanical properties. In polymer-based electrochemical technologies, these complexes are applied to solid-state lithium batteries, dye-sensitized solar cells, chemical sensors, and electrochromic devices.[1–4] These materials were also successfully used as a separation membrane for olefin/paraffin mixtures, using reversible interactions between metal ions and olefin molecules.[5] In particular, polymer electrolyte membranes with proton conducting properties have been extensively investigated for applications to fuel cells.[6–15]

Correspondence to: J. H. Kim (jonghak@yonsei.ac.kr).

Contract grant sponsors: Ministry of Knowledge Economy through the Manpower Development Program for Energy, New and Renewable Energy R and D Program; contract grant number: 2009T100100606.

Contract grant sponsors: Workforce Development Program in Strategic Technology of Korea Institute for Advancement in Technology (KIAT), Low Observable Technology Research Center program of the Defense Acquisition Program Administration and Agency for Defense Development.

Fuel cells produce electric power through a chemical reaction of fuel and oxygen, and thus they have been attracting significant attention as a clean source of energy. Polymer electrolyte membrane fuel cells (PEMFC) have been extensively studied for applications in electric vehicles, residential power sources, and portable devices. Perfluorinated polymer membranes containing sulfonic acid groups, e.g., Nafion, are widely acknowledged as an electrolyte membrane due to their excellent thermal, mechanical, and electrochemical properties. Great membrane properties stem from the structures in which the membranes consist, of a hydrophobic fluorocarbon backbone and hydrophilic sulfonic pendant side chains. However, many concerns have been raised for their use in fuel cell applications. For example, high cost, synthetic difficulty, toxic intermediates, loss of proton conductivity at high temperatures (>100°C), and high methanol crossover are serious drawbacks for practical applications in fuel cells. Therefore, there has been a great deal of research in the development of alternative proton conducting membranes to the perfluorinated membranes.[6–18]

Microphase separation of a copolymer can be used to create well-defined periodic microdomains of controlled morphology on the nanoscale. In particular, the use of a self-organized, nanophase-separated

structure can allow for a better control of both the sulfonation degree and the distribution of sulfonic acid groups in polymer electrolyte membranes. Therefore, the proton conducting properties of polymer electrolyte membranes with a phase-separated structure and self-organized ionic aggregates are higher than those of homogeneous materials.[19] The advantages of the use of a microphase-separated block copolymer include: control of the swelling of the ion conducting domains by the surrounding nonconducting domains, lowering of the methanol permeability due to decreased swelling, and high mechanical stability due to the inert matrix of nonsulfonated segments.[19–22]

Proton transport properties are strongly associated with the water uptake of membranes. Polymer electrolyte membranes with the higher degree of sulfonation show higher proton conductivity, but consequently higher water swelling, leading to their inadequate use in practical applications. Thus, crosslinking has been introduced as a solution to maintain a proper sulfonation level and to enhance the mechanical properties.[22–25]

In general, poly(styrene-*b*-butadiene-*b*-styrene) (SBS) triblock copolymer was crosslinked to improve its physical and mechanical properties.[26–28] For example, Mateo et al.[26] prepared crosslinked SBS using hexanediol dimethacrylate to increase transmittance through the visible light region, while retaining the regular structure. SBS membranes were also crosslinked with an aim to control proton conducting properties.[29,30] However, there has been no report on the SBS polymer electrolyte membranes crosslinked with proton conducting chains. Herein, we report on the crosslinked polymer electrolyte membranes based on SBS triblock copolymer and a sulfonated monomer, 2-sulfoethyl methacrylate (SEMA). SBS membranes were thermally crosslinked with SEMA in the presence of a thermal-initiator, 4,4′-azobis(4-cyanovaleric acid) (ACVA). The detailed properties of crosslinked SBS/SEMA membranes, e.g., ionic exchange capacity (IEC), water uptake, proton conductivity, structures, mechanical, and thermal properties, are reported in this article.

EXPERIMENTAL

Material

Poly(styrene-*b*-butadiene-*b*-styrene) (SBS, 30 wt % PS, M_w = 140,000 g/mol) and 4′-azobis(4-cyanovaleric acid) (ACVA) were purchased from Aldrich. 2-sulfoethyl methacrylate (SEMA, >90%) was purchased from Polysciences, Inc. All chemicals were used without further purification.

Membrane preparation

The crosslinked SBS/SEMA membrane was prepared by blending SBS and SEMA in THF. First, SBS was dissolved in THF for 60 min, and then SEMA was added to the SBS solution. The weight ratios of SEMA to SBS were changed from 12.5 to 50.0 wt %. The solution was stirred for 30 min. Next, the initiator, ACVA (5 wt % of the solution) was added to the solution, and then the solution was stirred at room temperature for 1 h for thorough mixing. Finally, the solution was cast onto a glass dish, which was covered with aluminum foil. The dishes were dried in an oven at 80°C for 48 h under N_2 atmosphere.

Ion exchange capacity

The ion exchange capacity (IEC) values of membranes were measured by the classical titration method. The membranes were soaked in 1.0*M* NaCl solution for 24 h before measuring IEC. The protons released due to the exchange reaction with Na ions were titrated against 0.01*M* standardized NaOH solution, using a phenolphthalein indicator. The IEC of the graft copolymer membranes was calculated using the following equation:

$$\mathrm{IEC(mEq/g)} = X \times N_{\mathrm{NaOH}}/\mathrm{Weight(polymer)} \quad (1)$$

where X is the volume of NaOH consumed and N_{NaOH} is the normality of NaOH. The reported IEC values were the mean of at least five measurements, and the average estimated error was ±6%.

Water uptake

Water uptake was determined by weighing vacuum dried membranes and fully equilibrated membranes with water after immersion in water for 24 h. The surface of the membrane sample was quickly wiped with an absorbent paper to remove the excess of water adhering to it and the sample was then weighed. The water uptake of membranes was determined from Eq. (2)

$$\mathrm{water\ uptake(wt\%)} = (W_w - W_d/W_d) \times 100 \quad (2)$$

where W_w and W_d are the weights of wet and dried membranes, respectively. The values of the water content reported are the mean of at least five measurements, and the average estimated error was ±8%.

Proton conductivity

A galvanostatic four-point probe method was used to measure the proton conductivity of membranes

using a home-made conductivity cell.[22,31,32] The ionic conductivity determined by the four-probe method is higher to some degree, but more accurate than that of the two-probe method, due to the minimization of contact impedance.[33] Before the measurement of proton conductivity, the prepared membranes were equilibrated with deionized water. Complex impedance measurements were carried out in the frequency range of 1 Hz–8 MHz at 25°C, using a ZAHNER IM-6 impedance analyzer. The impedance spectra of membranes can be used to generate Nyquist plots, and the proton conductivity was calculated from the plots. The impedance of each sample was measured five times to ensure good data reproducibility. The average estimated error was ±5%.

Characterization

FT-IR spectra of membranes were collected using an Excalibur Series FTIR (DIGLAB Co.) between the frequency ranges of 4000–400 cm^{-1} using the ATR facility. Wide angle X-ray scattering (WAXS) measurements were performed with a Rigaku D/max-RB apparatus (Tokyo, Japan). Data were collected from 5° to 60° at a rate of 1°/min. Transmission electron microscopy (TEM) pictures were obtained from a Philips CM30 microscope operating at 300 kV. For TEM measurements, a drop of dilute polymer solution with and without SEMA/ACVA at 0.5 ~ 1 wt % (the film thickness was 50–70 nm) was placed onto a standard copper grid. The samples were thermally crosslinked at 80°C for 48 h after staining with OsO_4 vapor. Small angle X-ray scattering (SAXS) data were measured at the 4C1 beamline at the Pohang Light Source (PLS), Korea. The operating conditions were set to a wavelength of 1.608 Å ($\Delta\lambda/\lambda = 1.5 \times 10^{-2}$), sample-to-detector distance of 2 m, beam size of 1×1 mm^2, and sample thickness of 1.5 mm. A 2D-CCD detector (Princeton Instruments Ins., SCX-TE/CCD-1242) was used to collect the scattered X-rays. Tensile evaluation was performed on a universal testing machine (UTM, a LR10KPlus Series) at a speed of 5 mm/min at room temperature. All the films were rectangular with a length of 2 cm and a width of 0.7 cm. The average thickness of the films was ~80 μm. The thermal properties of membranes were determined by thermal gravimetric analysis (TGA, Mettler Toledo TGA/SDTA 851e, Columbus, OH). TGA measurements were performed under a nitrogen atmosphere from room temperature to 700°C at a rate of 20°C/min. The amounts of membranes were determined as a weight loss percentage during heating.

RESULTS AND DISCUSSION

Preparation of crosslinked membranes

The reaction scheme for the preparation of crosslinked SBS/SEMA membranes is illustrated in Scheme 1. Neat SBS block copolymer is expected to exhibit a hexagonally packed cylinder morphology, because the volume fraction of PS is ~ 27%. The SBS membranes were thermally crosslinked with SEMA via chemical reaction between the aliphatic C=C bonds in SBS and the C=C bonds in SEMA. Since SEMA contains sulfonic acid groups, the crosslinked middle blocks will become proton conducting domains. Thus, the crosslinked triblock copolymer membrane consists of hydrophobic nonconducting PS blocks and crosslinked proton-conducting middle blocks. These amphiphilic membranes would molecularly self-assemble into continuous proton conducting domains of SEMA/butadiene chains interweaved with hydrophobic nanophase domains of PS blocks, providing a mechanism for facile proton transport through the membranes.[34,35]

Figure 1 shows the FT-IR spectra of pristine SBS (0 wt %) and crosslinked SBS/SEMA membranes with different concentrations of SEMA. Neat SBS (0 wt %) showed several weak bands at 1655, 1600, 1497, and 1445 cm^{-1}. The band at 1655 cm^{-1} is due to aliphatic C=C stretching vibration in the PB domain, whereas the other three bands are due to aromatic C=C stretching in the PS domain. Compared to the pristine SBS copolymer, the SBS/SEMA membranes exhibited strong absorption bands at 1724, 1212, 1157, and 1036 cm^{-1} and their intensities grew up with increasing SEMA concentrations. The absorption band at 1724 cm^{-1} is due to carbonyl oxygens (C=O) in SEMA, whereas the latter three bands result from the stretching vibrations of phenyl rings substituted with sulfonate groups and sulfonate anions attached to the phenyl ring.[27] The broad absorption band at 3420 cm^{-1} is attributed to the water bounded to ionic groups of the membranes.

IEC, water uptake, and proton conductivity

The IEC values of polymer electrolyte membranes are dependent on the content of sulfonic acid groups incorporated into the membranes, and are a very important property because of the direct indication of the actual ion exchange sites available for proton conduction. Figure 2 shows the IEC values of the SBS/SEMA membranes as a function of SEMA concentrations. Because sulfonic acid groups are contained in only SEMA, the IEC values almost linearly increased with SEMA concentrations. A maximum IEC of 1.4 meq/g was reached at 50 wt % of SEMA.

The water uptake of polymer electrolyte membranes is also an important property for proton

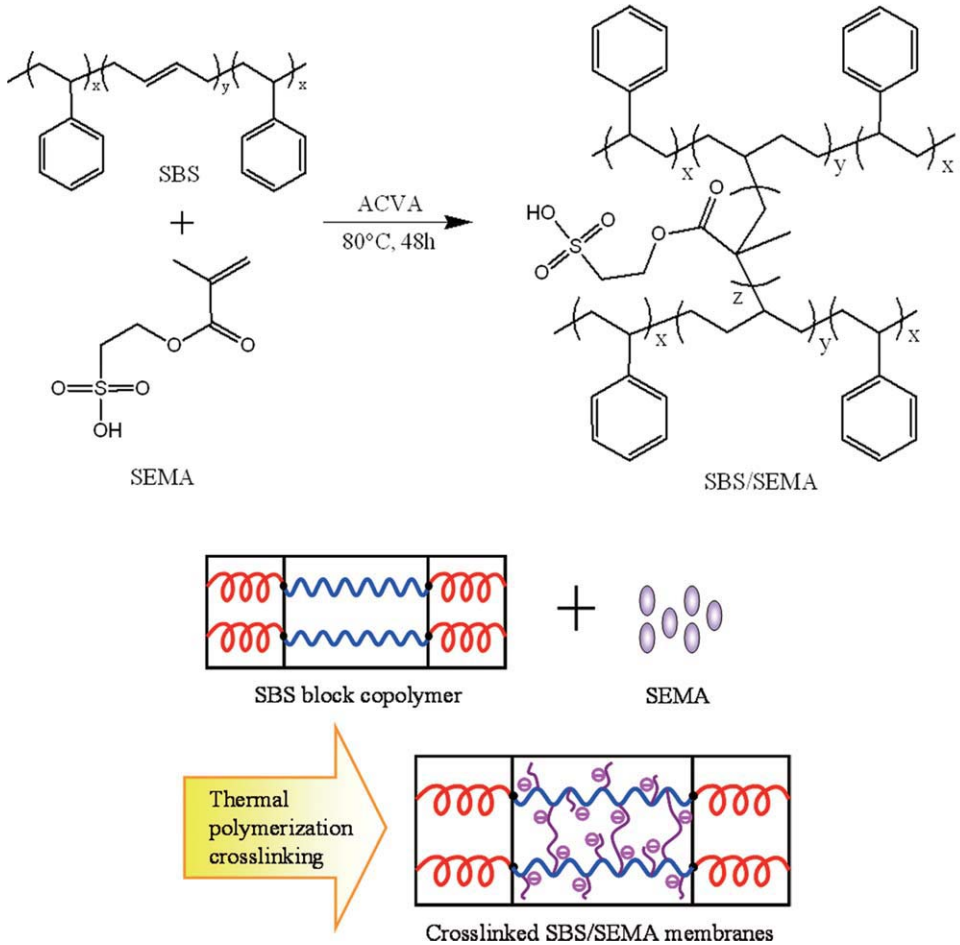

Scheme 1 Preparation procedure of crosslinked SBS/SEMA membranes. [Color figure can be viewed in the online issue, which is available at wileyonlinelibrary.com.]

conduction. Generally, the water uptake of an electrolyte membrane directly depends on the content of sulfonic acid groups, which are very hydrophilic, and thus higher contents of sulfonic acid group lead to higher water uptake. The water uptakes of SBS/SEMA membranes were measured at room temperature and are presented in Figure 3. A general behavior is that the water uptake increases with increasing

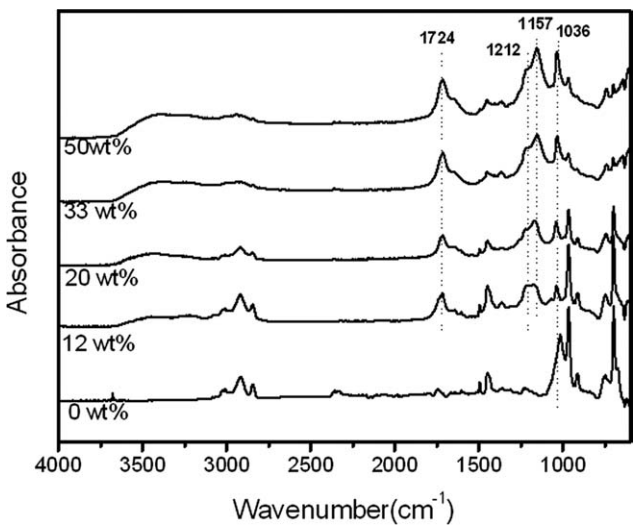

Figure 1 FT-IR spectra of crosslinked SBS/SEMA membranes with different SEMA content.

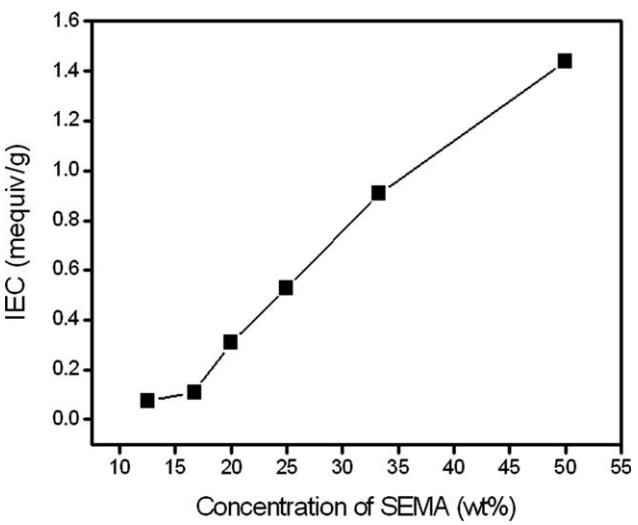

Figure 2 IEC of crosslinked SBS/SEMA membranes with different SEMA content.

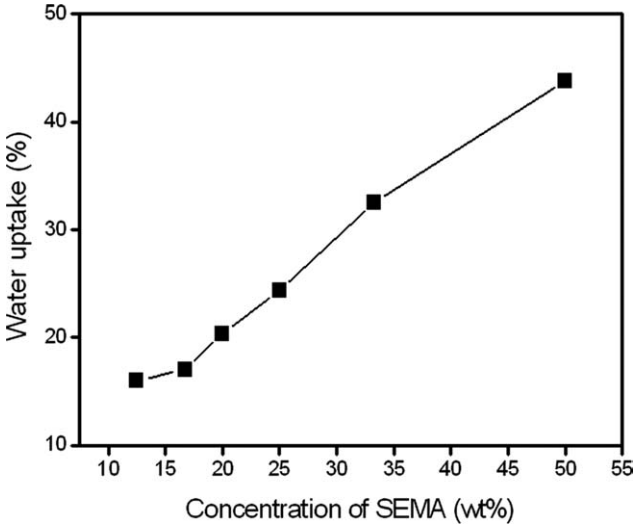

Figure 3 Water uptake of crosslinked SBS/SEMA membranes with different SEMA content.

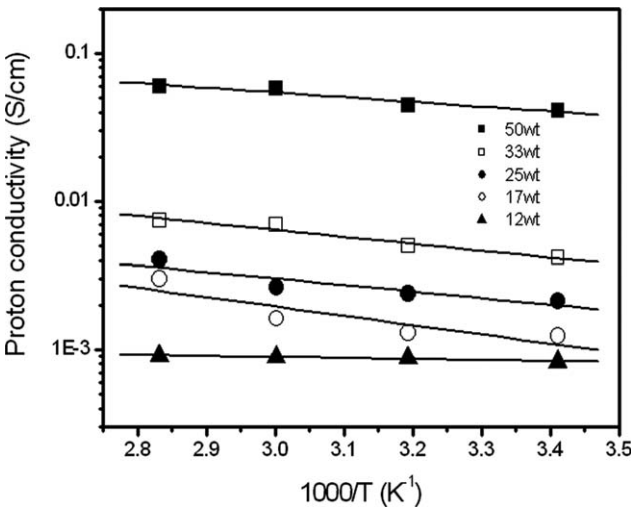

Figure 5 Temperature-dependent proton conductivity of crosslinked SBS/SEMA membranes with different SEMA content.

SEMA concentrations, because both properties are strongly related to the amount of sulfonic acid groups. The crosslinked SBS/SEMA membranes with 50 wt % of SEMA content exhibited a water uptake of 44%, which is comparable with that of Nafion 117 (40%).

Proton conductivity is one of the most important properties of polymer electrolyte membranes for fuel cells. The charge density of fuel cells strongly depends on proton conductivity, and thus the membranes with high proton conductivity are highly desired. The proton conductivities of crosslinked SBS/SEMA membranes were determined using a four probe method and are presented in Figure 4 as a function of SEMA concentrations. The proton conductivity gradually increased in proportion to the SEMA content up to 33 wt %, above which it abruptly jumped up from 0.004 to 0.04 S/cm. It is interesting because both the IEC values and the water uptake of SBS/SEMA membranes linearly increased with SEMA concentrations. This result suggests that the channels through which proton ions move are sufficiently formed only above 33 wt % of SEMA.

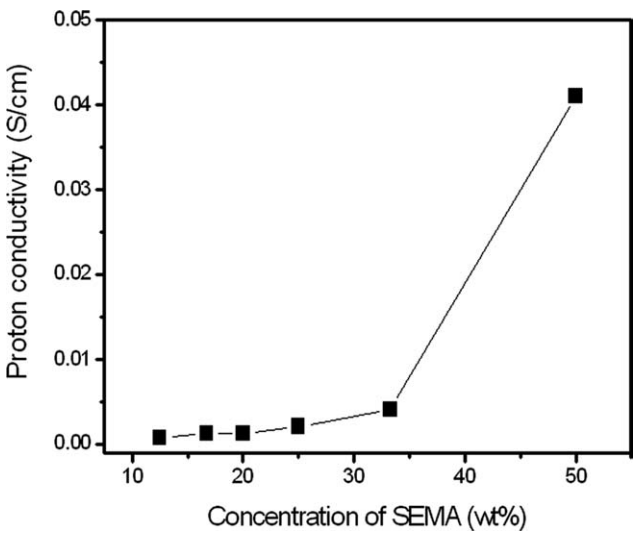

Figure 4 Proton conductivity of crosslinked SBS/SEMA membranes with different SEMA content at room temperature.

The proton conductivities of crosslinked SBS/SEMA membranes were also measured as a function of temperature and are provided in Figure 5. The membranes exhibited an increase of proton conductivity with temperature elevation, but the membrane with the lowest SEMA concentration (12 wt %) showed only a marginal change of conductivity with temperature variation. This implies that temperature-dependent proton conductivity is more sensitive to the concentration of sulfonic acid groups in crosslinked SBS/SEMA membranes. It can be explained by the fact that as temperature increases, the mobility of water, reorientation of polymer, and flexibility of polymer structure also increase.

Structure and morphology of membranes

WAXS is widely used as a powerful tool to investigate the structural changes of polymer electrolyte membranes, and thus the morphological structure of crosslinked SBS/SEMA membranes was analyzed by WAXS. The WAXS patterns for the crosslinked SBS/SEMA membranes with different SEMA concentrations are shown in Figure 6, where the intensity of X-ray scattering is plotted against the diffraction angle, 2θ. All the membranes exhibited a single

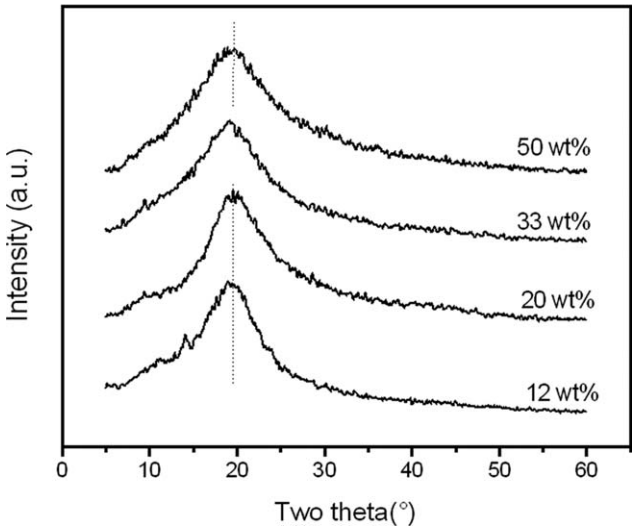

Figure 6 WAXS patterns of crosslinked SBS/SEMA membranes with different SEMA content.

broad amorphous band centered at 19.5°, irrespective of SEMA content. The Bragg *d*-spacing was calculated to be 4.5 Å for all crosslinked SBS/SEMA membranes. Although Bragg *d*-spacing was not significantly changed, the corresponding full width at half maximum (FWHM) was varied with SEMA concentrations, as shown in Table I. As can be seen in the table, the membranes showed a tendency of increasing FWHM with respect to SEMA content. This tendency can be explained by the fact that crosslinking/or grafting of SBS with SEMA chains alters the resulting molecular structure and physical network of SBS, leading to an increase of both the structural randomness of membranes and the perturbation of long-ranged spacing between the chains. This effect became more pronounced at higher SEMA concentrations.

TEM analysis was carried out to characterize the morphology of polymer electrolyte membranes. Figure 7 presents the TEM images of pristine SBS and SBS/SEMA membranes with different SEMA content. Because the membranes were stained with OsO_4 vapor, the dark regions represent butadiene domains, whereas the brighter regions are due to styrene or SEMA regions. The neat SBS block copolymer film exhibited a hexagonally packed cylinder morphology, corresponding to 27 vol % of PS [Fig. 7(a)]. Upon introduction of SEMA and crosslinking of membranes, cylinder morphology was disrupted to some degree, but the microphase separated morphology was retained [Fig. 7(b,c)]. The staining agent, OsO_4 is confined in only C=C bonds of butadiene domains, which are reduced with

TABLE I
FWHM Values of Crosslinked SBS/SEMA Membranes Determined by WAXS

SEMA concentration	12 wt %	20 wt %	33 wt %	50 wt %
FWHM	7.4	7.3	8.0	8.8

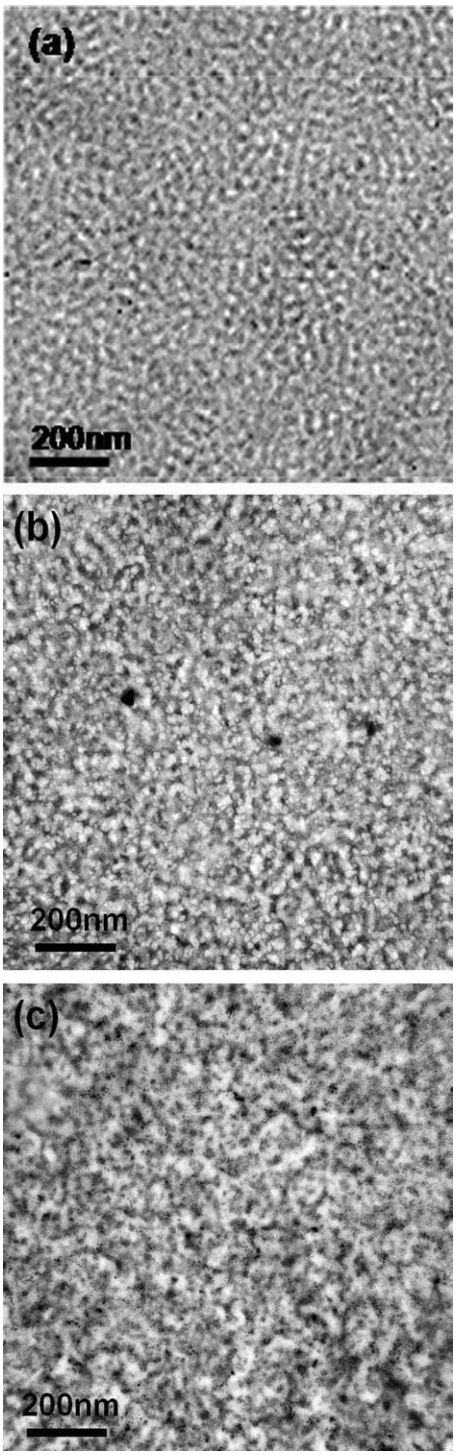

Figure 7 TEM images of (a) pristine SBS and crosslinked SBS/SEMA membranes with (b) 20 wt % and (c) 50 wt % of SEMA.

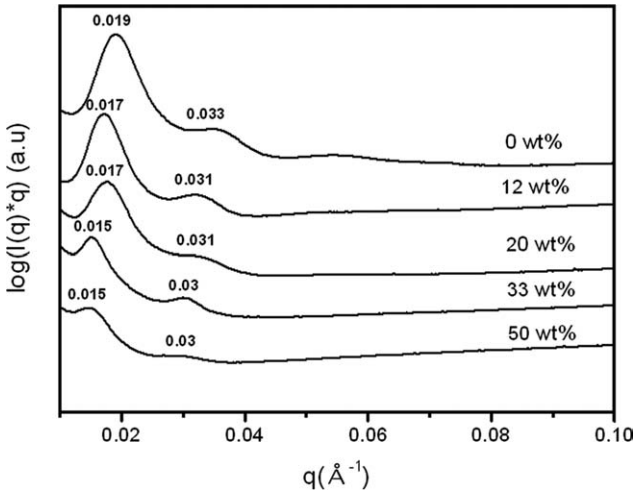

Figure 8 SAXS data of pristine SBS and crosslinked SBS/SEMA membranes with different SEMA content.

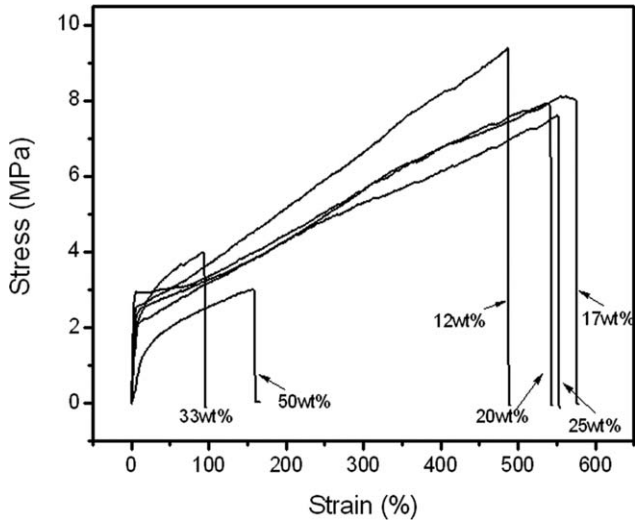

Figure 9 UTM data of crosslinked SBS/SEMA membranes with different SEMA content.

increasing SEMA concentration and crosslinking degree. Thus, the area of the dark domains is reduced upon the introduction of SEMA. These TEM images also showed that the crosslinked SBS/SEMA membranes exhibited a microphase separated morphology to allow for facile proton transport through the membranes.

SAXS has been well established as a experimental technique to complement the structural analysis obtained from the microscopy images, because it gives information over a large area.[36–38] Thus, SAXS has been employed to investigate the nano-structural transitions in the SBS block copolymer upon the introduction of SEMA and crosslinking, as shown in Figure 8. It is well established that block copolymer structure can be determined by SAXS from the q-values at the intensity maxima, e.g., 1, 2, 3, 4... for lamellar, $1, \sqrt{3}, \sqrt{4}, \sqrt{7}, \sqrt{9}$... for cylindrical, and $1, \sqrt{2}, \sqrt{3}, \sqrt{4}, \sqrt{5}$... for spherical morphologies.[36–38] The neat SBS block showed a hexagonally packed cylinder morphology, which is consistent with the TEM images of Figure 7. This morphology was not significantly changed up to 20 wt % of SEMA, above which the *q*-values at the intensity maxima were positioned with 1, 2, 3... This result seemingly indicates a lamellar morphology of the membranes, which was not clearly observed in the TEM image of Figure 7(c). The domain *d*-spacing values determined from the first peak using $2\pi/q$ continuously increased from 33 to 42 nm due to the volume increase of membranes.

Mechanical and thermal properties

Tensile evaluation was performed on the membranes using UTM at a speed of 5 mm/min, as shown in Figure 9. Tensile strength at break (MPa), elongation at break (%), and Young's modulus (MPa) for the crosslinked SBS/SEMA membranes with different SEMA concentrations are summarized in Table II. In general, a crosslinked structure results in the enhancement of mechanical properties of polymer electrolyte membranes. However, the mechanical properties of SBS/SEMA membranes such as strength and modulus did not linearly increase with SEMA concentrations. It is presumably due to the fact that SEMA contains sulfonic acid groups, which make the membranes more hydrophilic/hygroscopic, finally resulting in some loss of mechanical properties.

The thermal stabilities of crosslinked SBS/SEMA membranes were investigated by TGA as shown in Figure 10. All the membranes exhibited three step patterns for thermal degradation. The first weight loss of membranes was observed at around 100–200°C, which is mostly attributable to the loss of adsorbed water by the hygroscopic property of membrane. The second weight loss was observed at 250°C, which is generally correlated to the thermal

TABLE II
Mechanical Properties of Crosslinked SBS/SEMA Membranes

SEMA concentration (wt%)	Tensile strength (MPa)	Yield strength (MPa)	Young's modulus (MPa)	Elongation at break (%)
12	9.6	2.57	84.1	486
17	8.2	2.95	83.5	574
20	7.9	2.39	58.6	540
25	7.6	2.06	57.9	552
33	3.9	–	35.4	93
50	3	–	10.4	193

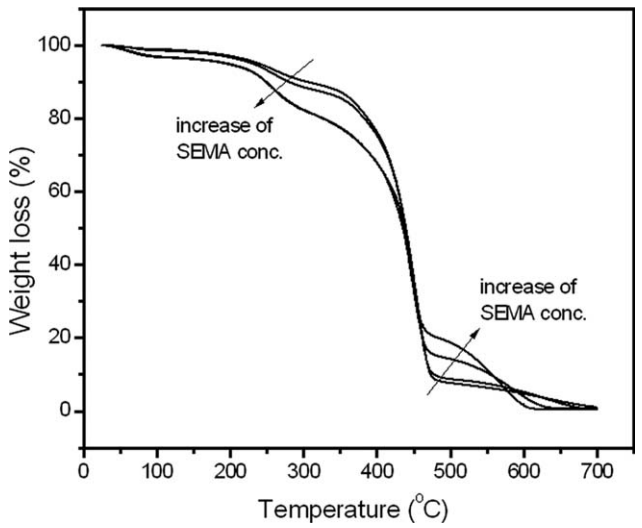

Figure 10 TGA of crosslinked SBS/SEMA membranes with different SEMA content.

degradation of sulfonic acid groups. As a result, this second weight loss became correlated with varying SEMA concentrations in membranes. The final weight loss started to appear at around 400°C, which is related to thermal degradation of main chain backbones. The third degradation was less correlated with the increase of SEMA concentrations probably due to the increase of crosslinking density in membranes. These TGA data suggest that the crosslinked SBS/SEMA membranes are thermally stable at least up to 250°C.

CONCLUSIONS

This work has demonstrated that polymer electrolyte membranes with controlled, crosslinked structure were prepared using SBS triblock copolymer and SEMA monomer with sulfonic acid groups. FT-IR spectroscopy showed that the SBS membranes were thermally crosslinked with SEMA using the thermal-initiator, ACVA. As expected, the IEC values and water uptake of SBS/SEMA membranes were increased in proportion to SEMA content in the membranes. However, the proton conductivity of membranes increased slowly, linearly with SEMA concentrations up to 33 wt %, above which it abruptly jumped up from 0.004 to 0.04 S/cm at room temperature. This result demonstrates that the channels through which proton ions move are sufficiently formed above 33 wt % of SEMA. WAXS analysis shows the "structureless" amorphous morphology of crosslinked SBS/SEMA membranes and the increase of structural randomness with SEMA concentrations. A microphase-separated morphology of membranes was observed and retained even after the introduction of SEMA and crosslinking of membranes, as revealed by TEM analysis. The characterization of crosslinked SBS/SEMA membranes by TGA demonstrated their high thermal stability up to 250°C. In addition, these membranes exhibited good mechanical properties, e.g., the SBS/SEMA membranes with 50 wt % of SEMA showed 10.4 MPa of Young's modulus and 193% of elongation at break, as determined by UTM.

References

1. Sirisopanaporn, C.; Fernicola, A.; Scrosati, B. J Power Sources 2009, 186, 490.
2. Zhang, P.; Li, G. C.; Zhang, H. P.; Yang, L. C.; Wu, Y. P. Electrochem Commun 2009, 11, 161.
3. Ahn, S. H.; Koh, J. H.; Seo, J. A.; Kim, J. H. Chem Comm 2010, 46, 1935.
4. Lee, K. M.; Suryanarayanan, V.; Ho, K. C. J Power Sources 2008, 185, 1605.
5. Kim, J. H.; Min, B. R.; Won, J.; Joo, S. H.; Kim, H. S.; Kang, Y. S. Macromolecules 2003, 36, 6183.
6. Daletoua, M. K.; Kallitsis, J. K.; Voyiatzis, G.; Neophytides, S. G. J Membr Sci 2009, 326, 76.
7. Farquet, P.; Padeste, C.; Borner, M.; Benyoucef, H.; Gursel, S. A.; Scherer, G. G.; Solak, H. H.; Saile, V. J Membr Sci 2008, 325, 658.
8. Reiter, J.; Velicka, J.; Mika, M. Electrochimica Acta 2008, 53, 7769.
9. Ismail, A. F.; Othman, N. H.; Mustafa, A. J Membr Sci 2009, 329, 18.
10. Kim, D. S.; Robertson, G. P.; Guiver, M. D.; Lee, Y. M. J Membr Sci 2006, 281, 111.
11. Mohd Norddin, M. N. A.; Ismail, A. F.; Rana, D.; Matsuura, T.; Mustafa, A.; Tabe Mohammadi, A. J Membr Sci 2008, 323, 404.
12. Tang, H.; Wan, Z.; Pan, M.; Jiang, S. P. Electrochem Commun 2007, 9, 2003.
13. Smitha, B.; Anjali Devi, D.; Sridhar, S. Int J Hydrogen Energy 2008, 33, 4138.
14. Smitha, B.; Sridhar, S.; Khan, A. A. J Power Sources 2006, 159, 846.
15. Ramani, V.; Kunz, H. R.; Fenton, J. M. J Membr Sci 2005, 266, 110.
16. Sambandam, S.; Ramani, V. J Power Sources 2007, 170, 259.
17. Gao, Y.; Robertson, G. P.; Guiver, M. D.; Jian, X. G.; Mikhailenko, S. D.; Wang, K. P. J Membr Sci 2003, 227, 39.
18. Xing, P. X.; Robertson, G. P.; Guiver, M. D.; Mikhailenko, S. D.; Kaliaguine, S. J Polym Sci A Polym Chem 2004, 42, 2866.
19. Vie, P.; Paronen, M.; Strømgard, M.; Rauhala, E; Sundholm, F. J Membr Sci 2002, 204, 295.
20. Haack, M.; Taeger, J.; Vogel, A.; Schlenstedt, C.; Lenk, K.; Lehmann, W. Sep Pur Tech 2005, 41, 207.
21. Yang, Y.; Shi, Z.; Holdcroft, S. Macromolecules 2004, 37, 1678.
22. Lee, D. K.; Kim, Y. W.; Choi, J. K.; Min, B. R.; Kim, J. H. J Appl Polym Sci 2008, 107, 819.
23. Mikhailenko, S. D.; Wang, K. P.; Kaliaguine, S.; Xing, P. X.; Robertson, G. P.; Guiver, M. D. J Membr Sci 2004, 233, 93.
24. Chen, J. H.; Asano, M.; Yamaki, T.; Yoshida, M. J Power Source 2006, 158, 69.
25. Xing, D.; Kerres, J. Polym Adv Tech 2006, 17, 591.
26. Mateo, J. L.; Calvo, M.; Bosch, P. J Appl Polym Sci 2003, 89, 2857.
27. Decker, C.; Viet, T. N. T. J Appl Polym Sci 2000, 77, 1902.

28. Li, L.; Chen, C. K.; Li, J.; Zhang, A. J.; Liu, X. Y.; Xu, B.; Gao, S. B.; Jin, G. H.; Ma, Z. J Mater Chem 2009, 19, 2789.
29. Won, J.; Park, H. H.; Kim, Y. J.; Choi, S. W.; Ha, H. Y.; Oh, I. H.; Kim, H. S.; Kang, Y. S.; Ihn, K. J Macromolecules 2003, 36, 3228.
30. Matsumoto, K.; Ozaki, F.; Matsuoka, H. J.; Polym Sci A Polym Chem 2008, 46, 4479.
31. Kim, Y. W.; Choi, J. K.; Park, J. T.; Kim, J. H. J Membr Sci 2008, 313, 315.
32. Kim, Y. W.; Park, J. T.; Koh, J. H.; Roh, D. K.; Kim, J. H. J Membr Sci 2008, 325, 319.
33. Lee, C. H.; Park, H. B.; Lee, Y. M.; Lee, R. D. Ind Eng Chem Res 2005, 44, 7617.
34. Zhang, M.; Russell, T. P. Macromolecules 2006, 39, 3531.
35. Hester, J. F.; Banerjee, P.; Won, Y. Y.; Akthakul, A.; Acar, M. H.; Mayes, A. M. Macromolecules 2002, 35, 7652.
36. Kim, J. H.; Lee, D. H.; Won, J.; Jinnai, H.; Kang, Y. S. J Membr Sci 2006, 281, 369.
37. Sakurai, S.; Aida, S.; Okamoto, S.; Ono, T.; Imaizumi, K.; Nomura, S. Macromolecules 2001, 34, 3672.
38. Epps, T. H., III; Bailey, T. S.; Waletzko, R.; Bates, F. S. Macromolecules 2003, 36, 2873.